Effects of Trailing-Edge Flap on Buffet Characteristics of a Supercritical Airfoil

B. H. K. Lee*
National Research Council, Ottawa, Ontario, K1A 0R6, Canada

The buffet characteristics of a 16% thickness-to-chord ratio supercritical airfoil were investigated in the Institute for Aerospace Research (IAR) High Reynolds Number Two-Dimensional Test Facility. The trailing-edge flap dimension was 13.5% chord and it was deflected at various angles to study the effect of modifying the downstream pressure on controlling flow separation over the airfoil. The unsteady normal force was measured and the buffet boundary was determined from the divergence of the fluctuating normal force. The investigation was conducted quite deep into the buffet regime. Spectral analyses of the normal force were carried out and the frequencies of shock-wave oscillations were measured. They were found to be Mach-number dependent and varied between 50–80 Hz for $M = 0.612$ to 0.792. The effects of varying the flap angles on the shock-wave position and drag of the airfoil were also investigated. Results for an off-design Mach number of 0.612 were given in some detail.

Nomenclature

b = model span
C_D = drag coefficient from wake integration
C_L = lift coefficient from balance measurements
$C_{L\max}$ = maximum lift coefficient
C_N = fluctuating normal-force coefficient from balance measurements
C'_N = rms value of normal-force coefficient
C_p = pressure coefficient
$C_{p\mathrm{TE}}$ = trailing-edge pressure coefficient
c = chord length
M = Mach number
M_D = drag rise Mach number
M_{DES} = design Mach number
q_∞ = freestream dynamic pressure
x = distance measured from airfoil leading-edge
x_s = shock-wave position
α = angle of incidence
δ = flap angle, positive downwards

I. Introduction

IN performing maneuvers inside the subsonic and transonic flight envelope, fighter aircraft often fly in the buffet regime for a significant amount of time. The buffet loads due to flow separation on the wing may cause serious fatigue problems and have an important impact on the structural integrity of the aircraft. In addition, maneuverability, performance, and handling qualities are often degraded. Delay of separation or increasing the airplane buffet onset normal-force coefficient to as large a value as possible is highly desirable.

Some early flight tests showed buffet could be alleviated or reduced through deflections of leading- and trailing-edge flaps. The results reported by Monaghan and Friend[1] were for the F-8C aircraft having wing section designed for subsonic flows, whereas the F-104 test aircraft used in Friend and Sefic's[2] investigation has supersonic airfoil design. In both cases, the wing was fairly thin. The effectiveness of using leading- and trailing-edge flaps for buffet alleviation were quite different in the two aircraft configurations. The results showed that for the F-8C leading-edge flaps were more effective, whereas for the F-104 the use of trailing-edge flaps gave better improvements in raising the buffet boundaries.

Aside from the two earlier studies with airfoils of conventional design, it appears that little or no research has been carried out on the use of flaps to control buffet of supercritical airfoils. To gain better insight into the effects of flaps on buffet intensities and delay of buffet onset at transonic conditions, flight tests or wind-tunnel investigations of supercritical airfoils with flaps are required. An understanding of the manner in which a flap can modify flow separation over the airfoil is useful in assessing effectiveness or feasibility of deploying a flap as a passive means of buffet control.

An investigation on the effects of a trailing-edge flap on buffet characteristics of a 16% thick supercritical airfoil was carried out in the IAR High Reynolds Number Two-Dimensional Test Facility. The airfoil was used in a previous joint IAR-Boeing Canada (de Havilland Division) research and development program in the study of airfoil design for drag reduction.[3] The design conditions for this airfoil were for a cruise Mach number of 0.72 and lift coefficient of 0.6. The original airfoil was modified by replacing the rear section with a trailing-edge flap of dimension approximately 13.5% chord. The installation of a leading-edge flap was considered to be much more complex and would alter the airfoil design characteristics. To control separation, the simplest way is to change the downstream pressure by use of a trailing-edge flap.

In an earlier paper,[4] some results from this investigation were described. Buffet onset boundaries with different flap-deflection angles were given. Most of the results on the characteristics of the buffet flow were presented at the design Mach number. In this paper, some further results are described and behavior of the flow at an off-design Mach number of 0.612 is discussed in some detail.

II. Model, Instrumentation, and Data Processing

The airfoil was made of aluminum having a chord of 12 in. and a span of 15 in. The thickness-to-chord ratio was 16%. The flap dimension was approximately 13.5% chord, and the trailing-edge thickness was 0.1% chord. There were 79 pressure orifices on the model surface for static pressure measurements: 43 of them were located on the airfoil upper surface and 23 on the lower surface. On the flap, there were 13

Received May 3, 1990; revision received Jan. 22, 1991; accepted for publication Feb. 4, 1991.

*Senior Research Officer, High Speed Aerodynamics Laboratory, Institute for Aerospace Research. Member AIAA.

pressure orifices with six on either side and one at the trailing edge. Their locations on the airfoil are shown in Fig. 1. The drag of the airfoil was obtained using a traversing wake rake with pitot probes at four spanwise locations that were approximately 18 in. downstream of the airfoil trailing edge. In this experiment, only the two centrally located probes were used and their average was taken for drag measurements.

The lift and pitching moment were determined from a sidewall balance. In addition to the steady-state values of the balance outputs, the fluctuating quantities were also measured. The rms value of the normal force is presented in nondimensional form given by

$$C'_N = N_{\text{rms}}/q_\infty bc \qquad (1)$$

Spectral analyses of the balance outputs were also performed. The signal was sampled at 1.6 kHz and analyzed digitally on a computer using the IEEE routine Periodgram Method for Power Spectrum Estimation (PMPSE)[5] to give power spectra and autocorrelation functions. A fast Fourier transform (FFT) block size of 256 and signal duration of 2 s were chosen in all of the analyses. A few longer duration runs of 10 s were performed and an FFT block size of 1024 was used.

As reported in Ref. 4, windoff tests on the response of the force balance to impulse excitation were carried out and four natural frequencies were detected at about 140, 215, 320, and 360 Hz. These were much larger than the peak excitation frequencies observed under buffet conditions that varied from approximately 50 Hz at $M = 0.612$ to 80 Hz at $M = 0.792$.

Distributed suction was applied through porous plates to regions of the tunnel side walls in the vicinity of the model. The amount of suction was selected so as to minimize any three-dimensional effects.

All of the tests were performed at a chord Reynolds number of approximately 20×10^6 with free transition. At design conditions, flow visualization using a thin film of oil containing a dye that fluoresced in ultraviolet light showed transition to occur on the upper surface at less than 5% chord from the leading edge. The Mach numbers in this investigation varied between 0.612–0.792 and the flap angle settings were $\delta = 0$, 4, 8, 14, −4, and −8 deg. The standard convention of positive flap deflection in the downward position and negative in the upward position was adopted. The maximum value of the angle of incidence was 10 deg.

III. Results and Discussions

A. Lift and Normal-Force Fluctuations from Balance Measurements

For this supercritical airfoil, it is noted from the C_L vs α curves that up to moderate angles of attack and M greater than the drag rise value M_D (determined from the criterion $dC_D/dM = 0.1$) at design conditions, C_L does not usually reach a maximum. However, below M_D a value of $C_{L\max}$ is detected. The C_L vs α curves at M_{DES} are shown in Fig. 2 for different δ. A $C_{L\max}$ is detected in all cases and the effect of the flap is to shift the curves either upwards to the left or downwards to the right depending on the sign of the flap angles. The value of α where $C_{L\max}$ occurs decreases as δ changes from negative to positive values. It varies from approximately 4.8 deg at $\delta = -8$ to 2.4 deg at $\delta = 14$ deg. The increase in lift for positive flap angles is quite significant. This is also true for Mach numbers below and above its design value as discussed in Ref. 6. At higher M, a $C_{L\max}$ is usually not detected and the C_L vs α curves are similar to those shown in Fig. 3 for $M = 0.772$.

The effects of changing flap angles on the fluctuating normal force were also given in Ref. 6 where results of C'_N variations

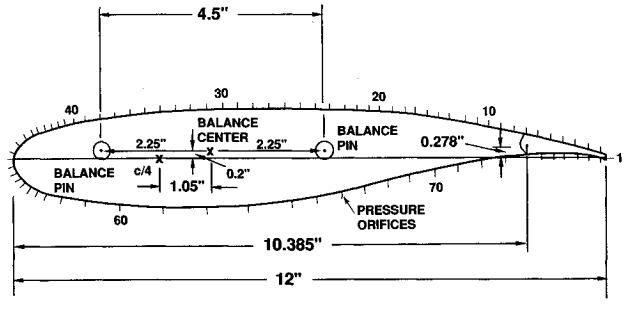

Fig. 1 Schematic of 16% thickness-to-chord ratio supercritical airfoil.

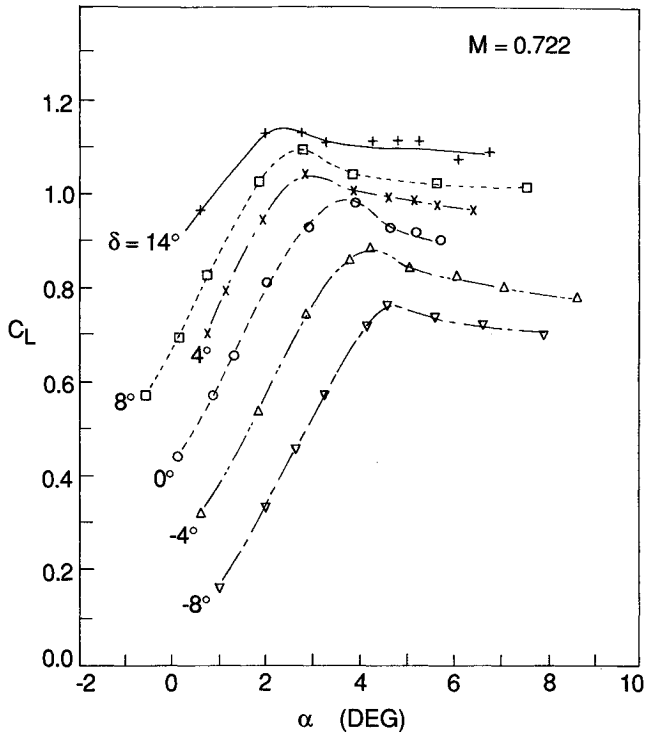

Fig. 2 C_L vs α at $M = 0.722$ and various flap angles.

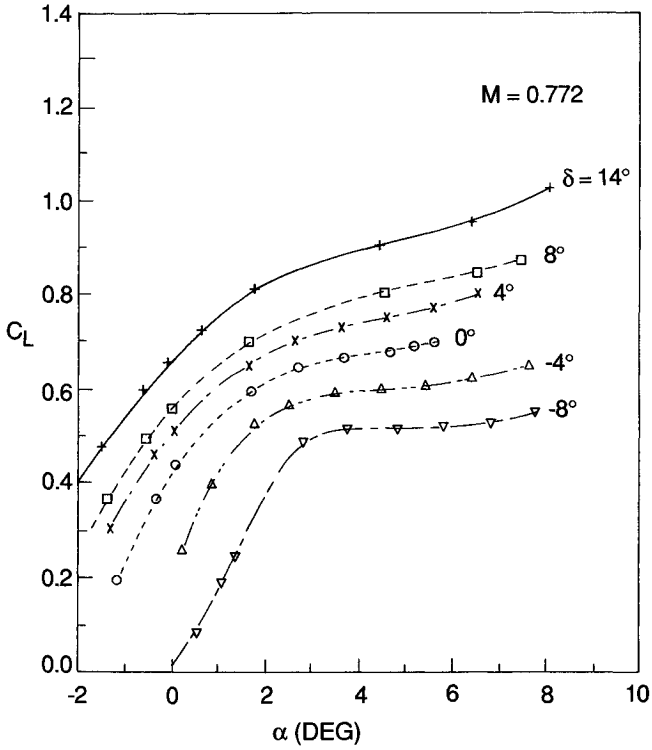

Fig. 3 C_L vs α at $M = 0.772$ and various flap angles.

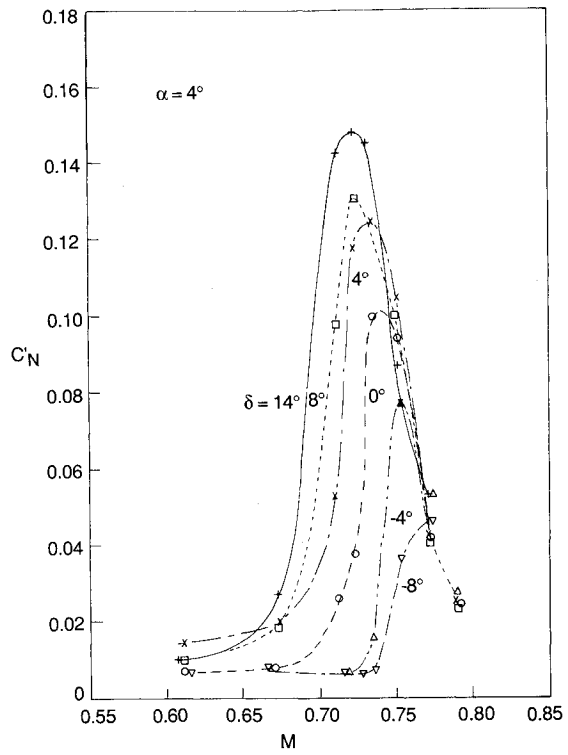

Fig. 4 C'_N vs M at $\alpha = 4$ deg and various flap angles.

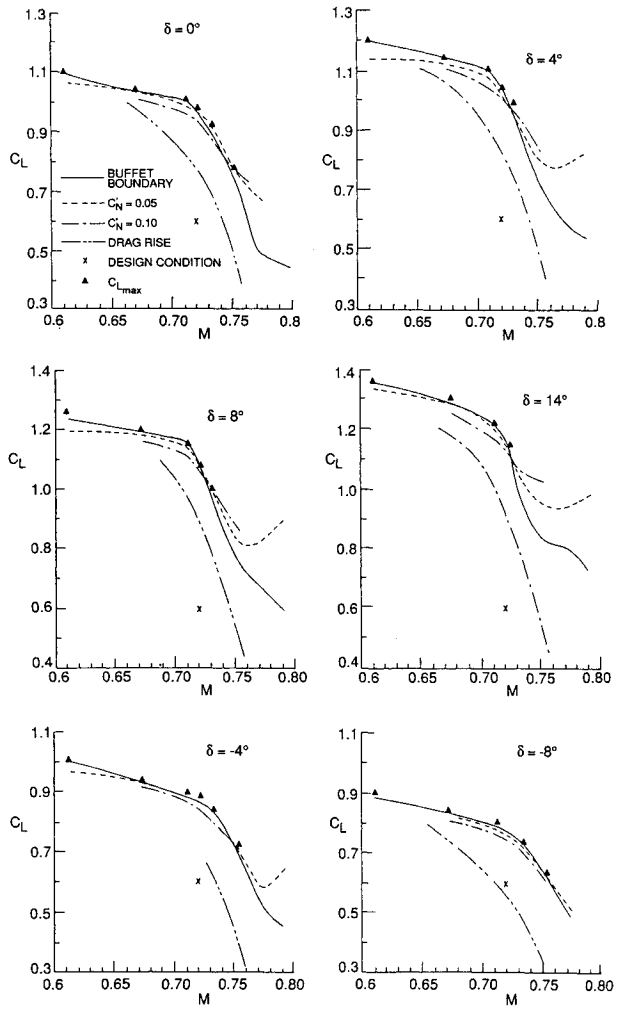

Fig. 5 Buffet boundaries for various flap angles.

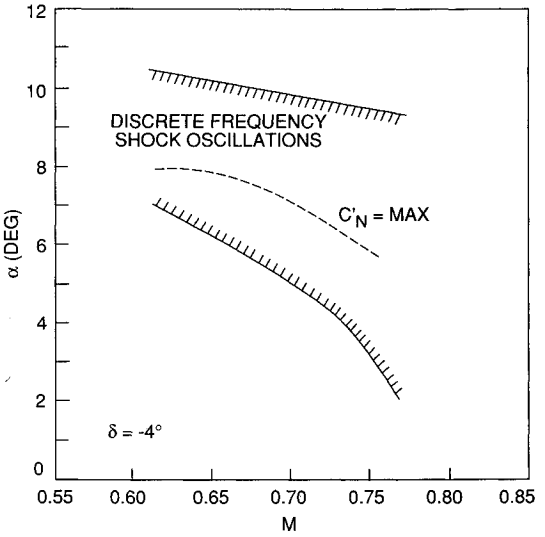

Fig. 6 Region of discrete frequency shock-wave oscillations at $\delta = -4$ deg.

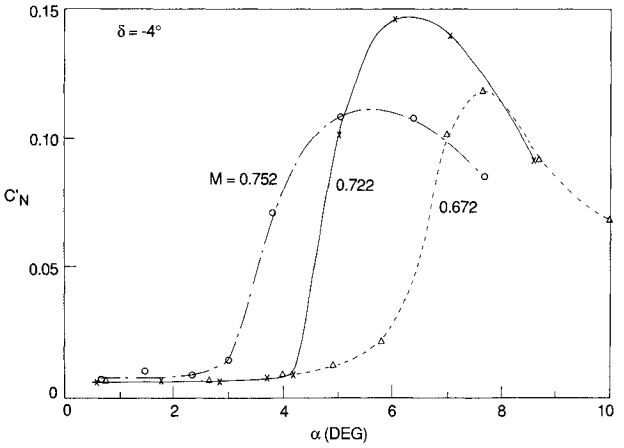

Fig. 7 Variations of C'_N with α at $\delta = -4$ deg.

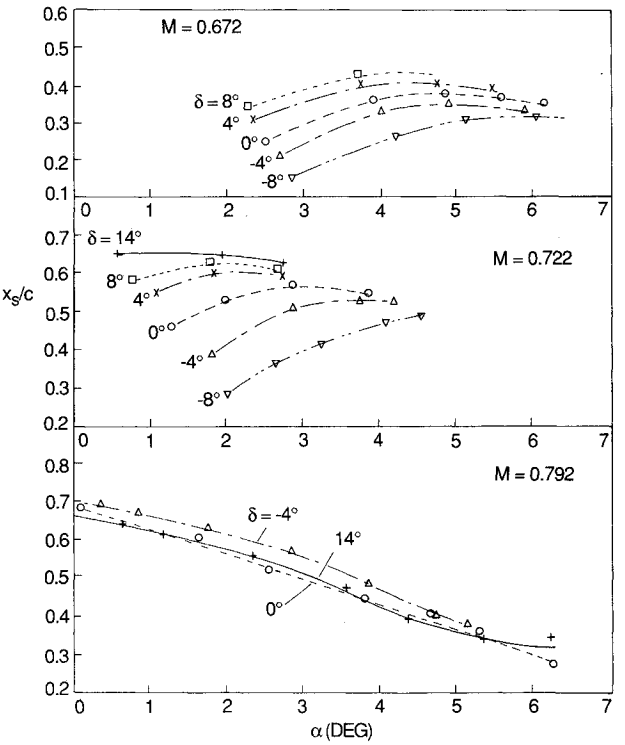

Fig. 8 Shock positions vs α for different values of δ at $M = 0.672$, 0.722, and 0.792.

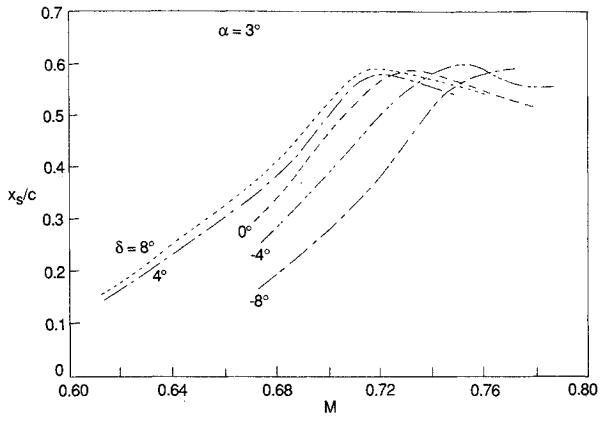

Fig. 9 Shock positions vs M at α = 3 deg for various flap angles.

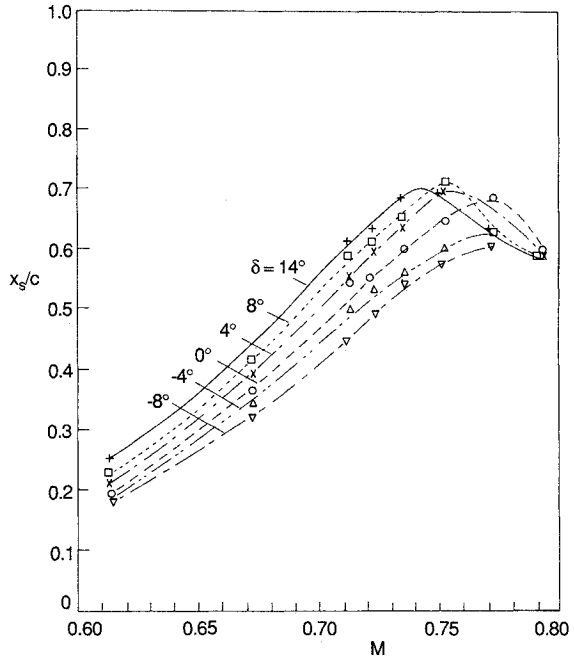

Fig. 10 Shock positions at buffet onset vs M for various flap angles.

with C_L for different M were shown. When C'_N is plotted against α, it is found that for M less than M_D = 0.75, C'_N reaches a maximum and then decreases with further increase in α. For larger M, the curves of C'_N increase monotonically with α with much smaller magnitudes.

To show the behavior of C'_N with M for different flap angles, results are given in Fig. 4 at α = 4 deg. Similar curves can be obtained for different α. For a given δ, C'_N increases with M and reaches a maximum. Its magnitude increases with positive δ and decreases with negative δ. Also, changing δ from negative to positive angles results in a smaller value of M where the maximum of C'_N occurs.

B. Buffet Boundaries

To determine the C_L at buffet onset, the procedure used is to obtain a smooth C'_N vs C_L curve either by the use of a spline or fitting manually. C_L at buffet is then determined by noting the point on the curve with a slope of dC'_N/dC_L = 0.1.[4] This value is arbitrarily chosen. When buffet onset is primarily due to trailing-edge separation, the results are found to be consistent with those derived using the trailing-edge pressure divergence criterion. Experience at IAR in testing supercritical airfoils shows that it is more convenient to use this technique to determine buffet onset. Installation of a pressure orifice close to or at the trailing edge to measure pressure

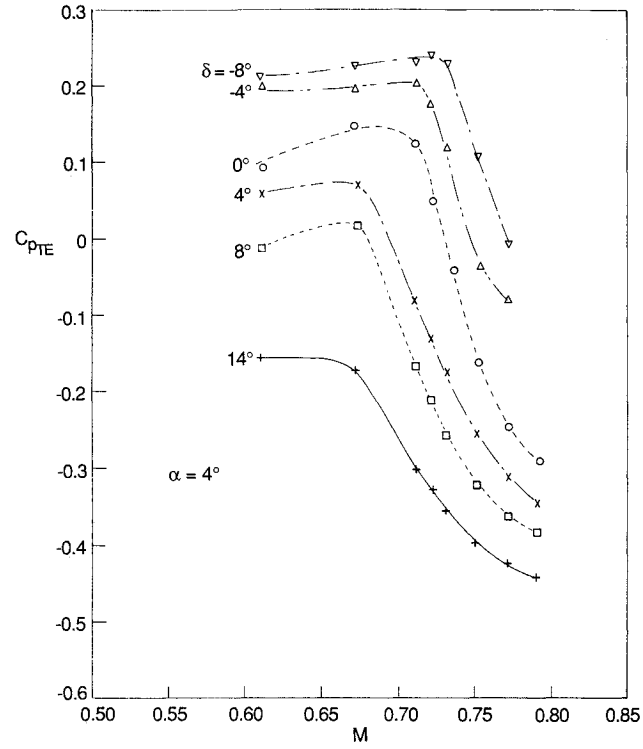

Fig. 11 $C_{p_{TE}}$ vs M at α = 4 deg for various flap angles.

divergence is cumbersome and often not feasible for airfoils with thin trailing edge. Also, it is often necessary to obtain trailing-edge pressure data over a wide range of incidence below buffet onset in order to define a baseline to locate α when trailing-edge pressure divergence occurs.

For conventional airfoils, it is often possible to designate in the C_L vs M plot regions of mild, moderate, or heavy buffeting. For supercritical airfoils such as the one investigated in this paper, buffet onset occurs so close to $C_{L\max}$ for M near or less than M_{DES} that it is not too meaningful to assign a degree of severity in the $C_L - M$ buffet plot, except when M is greater than some value, for example, M_D for this particular airfoil. Figure 5 shows the buffet onset boundary at different values of δ together with curves for two buffet intensities expressed in terms of constant C'_N. At δ = 0 deg, the curves lie below the buffet onset boundary at Mach numbers less than 0.72 and 0.75 for C'_N = 0.05 and 0.1, respectively. This is due to the behavior of the C'_N variations with C_L, where for $M < 0.75$ a decrease in C_L is detected when C'_N increases above its value at buffet onset.[4] For higher Mach numbers, the curves lie above the buffet onset boundary since C'_N increases with C_L monotonically. Also shown in Fig. 5 are the values of $C_{L\max}$ for those values of M where a maximum in C_L can be detected. For positive δ, the curves for C'_N = 0.05 and 0.1 cross the buffet boundary at M near 0.72, while for negative δ the value of M is close to 0.75.

It is seen that the buffet boundary curves can be raised appreciably and there are large increments in lift with positive changes in δ. C_L at buffet onset decreases rapidly for $M > M_{DES}$. At M = 0.75, which corresponds to the drag rise Mach number M_D at design C_L, this airfoil shows small gains in the buffet boundary by the use of flaps. Further increase in Mach number again shows an increase in the lift before encountering buffet. The drag-rise curves are also included in these figures and they are described in Sec. IIIE.

Spectral analyses[7] of the balance normal force have shown shock oscillations at frequencies 50–80 Hz for M = 0.612 to 0.792. They have been identified in a related study[8] on periodic shock motion as due to shock-boundary-layer interaction. In that investigation, a model of the self-sustained shock oscillations for the Bauer-Garabedian-Korn (BGK) No.

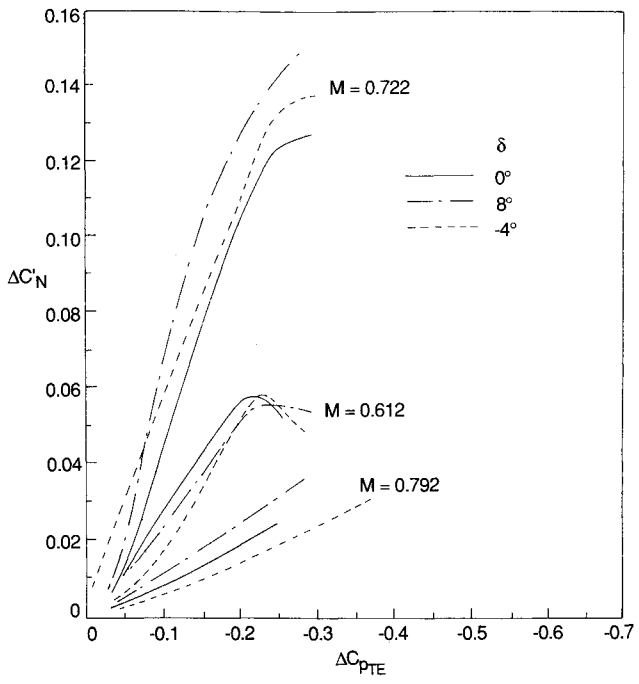

Fig. 12 $\Delta C'_N$ vs ΔC_{pTE} at M = 0.612, 0.722, and 0.792 and δ = −4, 0, and 8 deg.

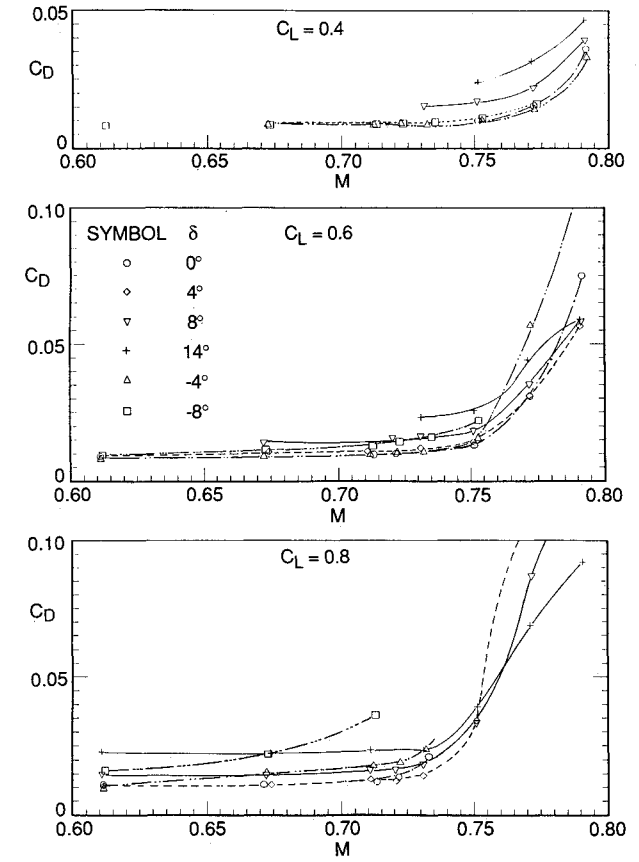

Fig. 13 C_D vs M at C_L = 0.4, 0.6, and 0.8 for various flap angles.

1 supercritical airfoil was proposed. The propagation velocity of the pressure disturbance due to the shock motion was measured experimentally. Using this velocity, the oscillating shock frequencies were calculated and they were found to be in good agreement with the measured values.

The normal-force power spectra[7] show that beyond the buffet onset boundary, the shock wave strengthens as α is increased. For a given M, there is an α above which the shock starts to weaken. A maximum value of α can be found where periodic shock motion is not detected. The flow conditions when shock oscillations occur are shown in Fig. 6 for $\delta = -4$ deg. The variations of C'_N with α for this δ are given in Fig. 7 for three Mach numbers, and they show that the value of α where C'_N is a maximum decreases with increasing M. The locations inside the shock oscillation region when C'_N reaches a maximum are shown in Fig. 6. Results for other values of δ show similar behavior.

C. Shock-Wave Positions

When the shock wave is oscillating its locations determined from C_p plots falls within the range of positions that occur during one pressure scan cycle of approximately 2.5 s. At severe buffet conditions locating the shock position is difficult. The manner in which shock position is measured in Ref. 9 is followed in this study and there is a certain degree of arbitrariness in this definition for large oscillating shock motion. However, the results using Ref. 9 definition of the shock position are consistent and measurements are relatively easy to carry out.

The effects of δ on shock position x_s/c are shown in Fig. 8 for three values of M. Except for the highest M tested at 0.792, which shows x_s/c to decrease with α, it is seen from the results for the other two M values that x_s/c increases with α initially and reaches a maximum before decreasing slowly. Except for large M, the effect of a trailing-edge flap is to move the shock position further downstream for positive δ and upstream for negative δ by varying the pressure behind the shock wave. The shock position is difficult to measure for high M. Only data for three values of δ at M = 0.792 are shown. The results for other δ indicate the shock position is quite similar for all positive δ, while for negative δ the shock occurs further downstream in contrast to an upstream movement for the lower M cases.

The variations of x_s/c with M is illustrated in Fig. 9 for α = 3 deg. The curves show the shock position to move downstream with increasing M until a maximum x_s/c is reached. From then onwards it moves gradually upstream. Similar trends are observed when the shock locations at buffet onset are plotted against M for various flap angles as shown in Fig. 10. At higher M (e.g., 0.792), the measurements of the shock location become difficult and are not very accurate.

D. Trailing-Edge Pressure Measurements

In this investigation, the trailing-edge pressure was measured as the airfoil incidence was increased to fairly large values beyond the buffet onset value. Some of the results presented in Ref. 6 are replotted here in the form of C_{pTE} vs M as shown in Fig. 11. The incidence α is fixed at 4 deg, and the effect of varying δ is illustrated. Similar curves are obtained for other values of α. The value of M where divergence of C_{pTE} at a given α can be determined from this type of plot.

From the trailing-edge pressure coefficient vs α or C_L plots, buffet severity can be represented by ΔC_{pTE}. This is obtained by noting the value of the trailing-edge pressure C_{pTEdiv} when divergence occurs (onset of buffet). As the airfoil moves deeper into the buffet regime, buffet severity can be measured in terms of C_{pTE} as

$$\Delta C_{pTE} = C_{pTE} - C_{pTEdiv} \tag{2}$$

The buffet intensity from normal-force fluctuation measurements is denoted in terms of C'_N as

$$\Delta C'_N = C'_N - C'_{NB} \tag{3}$$

where C'_{NB} denotes the value of C'_N at buffet onset. Figure 12 shows the relationship between $\Delta C'_N$ and ΔC_{pTE} for three values of M, namely, at M_{DES} and two values of M above and below M_{DES}. Only data using three values of δ are shown in order that the figure will not be unduly crowded. There is a

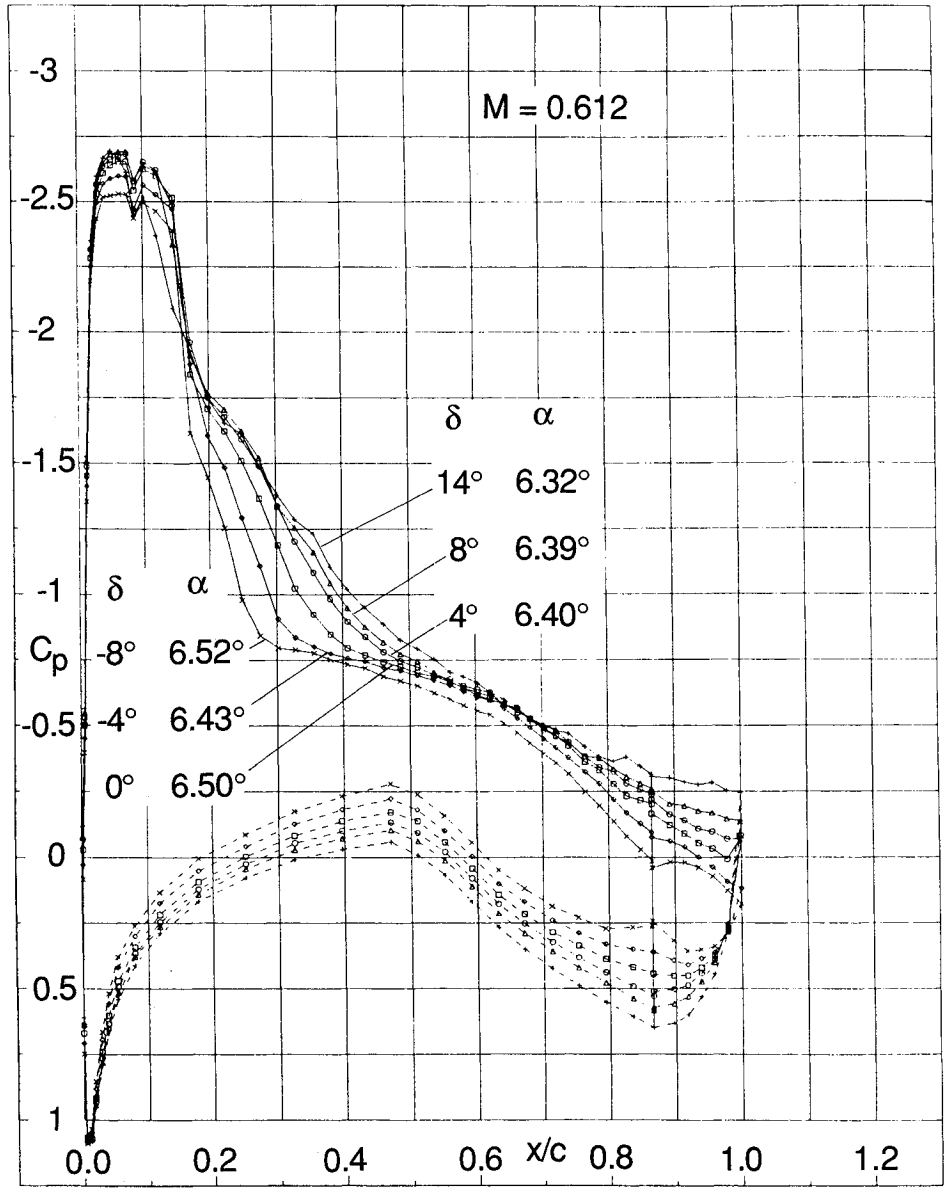

Fig. 14 C_p distributions at $M = 0.612$ for various flap angles.

maximum in $\Delta C'_N$ for the lower values of M tested, and this is due to an easily detectable C'_N maximum in the graphs plotted against C_L or α. At higher M, C'_N maximum is difficult to locate. From observing the results for other M values tested, it was noted that in the neighborhood of M_{DES} much larger changes in $\Delta C'_N$ with ΔC_{pTE} occur than at M lower or higher than M_{DES}. In the range of M near M_{DES}, the effects of flaps result in larger $\Delta C'_N$ changes with ΔC_{pTE}. The results for M smaller or greater than M_{DES} do not show any particular trend of the effect of the flaps on $\Delta C'_N$.

E. Drag Measurements

The drag polar was determined from wake measurements and at the design C_L, M_D (using a criterion based on a value of $dC_D/dM = 0.1$) was 0.75.

At the design C_L of 0.6, C_D vs M is plotted in Fig. 13. Below M_D, small flap angles ($\delta = \pm 4$ deg) do not increase the drag significantly. However, the drag of the airfoil with 8- and 14-deg flaps shows a fairly large increase above that for $\delta = 0$ deg. For off-design conditions at $C_L = 0.4$, the increase in drag for the 8- and 14-deg flaps are quite large. At $C_L = 0.8$, drag increase for negative flap angles is much larger than for positive angles of the same magnitude.

F. Results at Off-Design Mach Number

In Ref. 4, some results on the characteristics of this airfoil at the design Mach number were given. In this paper, the behavior of the airfoil at off-design conditions are discussed and the Mach number chosen is 0.612.

The static pressures are shown in the form of C_p plots given in Fig. 14. The profiles are taken from pressure scans close to $\alpha = 6.5$ deg. The pressure irregularity at $x/c = 0.087$ was due to a partially blocked orifice. The shape of the pressure profile between x/c 0.2–0.4 for positive δ is typical for airfoils when shock-induced separation with reattachment occurred. This type of flow separation for supercritical airfoils was studied and discussed in Ref. 10.

The trailing-edge pressure variations with α as the buffet regime is penetrated is shown in Fig. 15. The values of the α indicated in Fig. 14 are marked in Fig. 15 as "a," "b,". . . "f." It is seen that at $\delta = -8$ deg, the airfoil is not experiencing buffet and at $\delta = -4$ deg, the value of α is very close to that at buffet onset. For the other values of δ the airfoil is operating inside the buffet regime.

The corresponding variations of C'_N with α is shown in Fig. 16. The curves are displaced by 0.02 of an unit upwards to avoid overlapping. Using the divergence of C'_N as the buffet

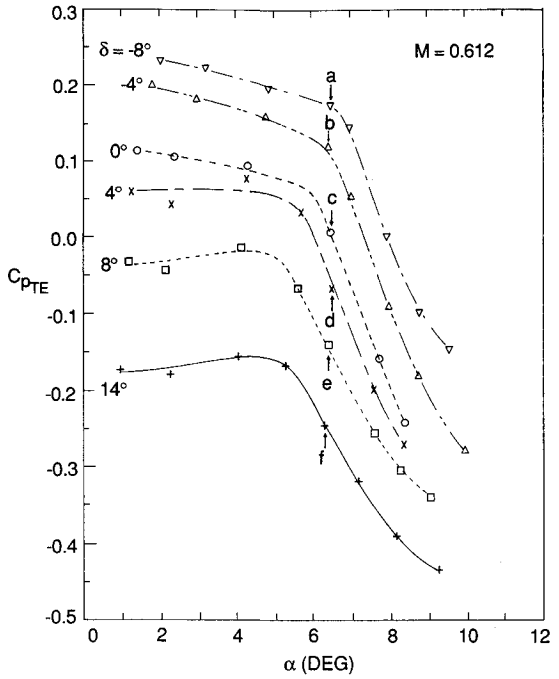

Fig. 15 C_{pTE} vs α at $M = 0.612$ for various flap angles.

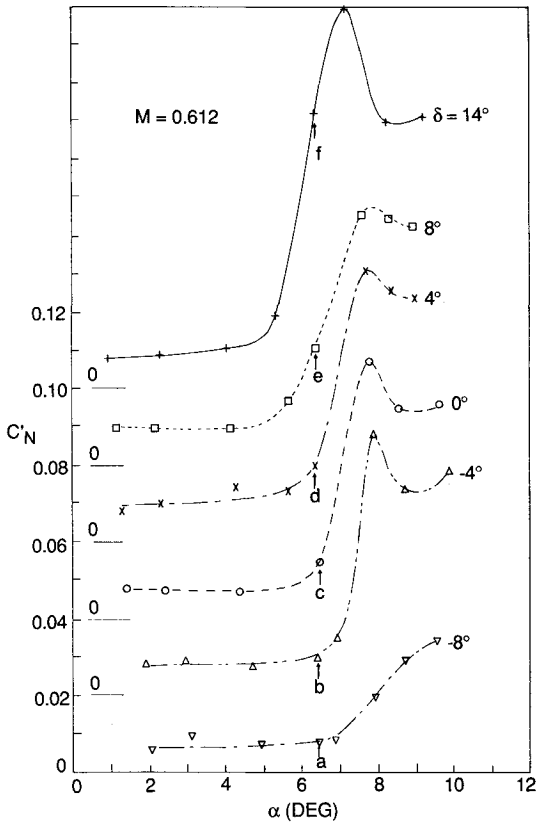

Fig. 16 C'_N vs α at $M = 0.612$ for various flap angles.

onset criterion, it can be seen from this figure that the airfoil is operating at buffet conditions for δ equal or greater than 0 deg. The peak in C'_N is a characteristic behavior when a $C_{L\max}$ is present.

The corresponding power spectra of the balance normal force are shown in Fig. 17. They are obtained using an FFT block size of 256 and a signal duration of 2 s. The curves are displaced 10 db downwards so that they will not overlap. The appearance of a shock wave with frequency of approximately 50 Hz begins at a value of $\delta = 0$ deg and the intensity of this shock increases with increasing δ.

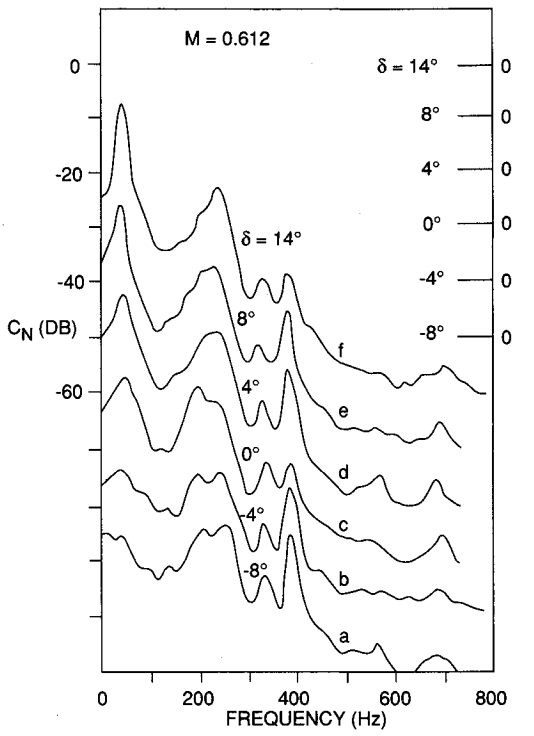

Fig. 17 Power spectra of balance normal force at $M = 0.612$ and α approximately 6.5 deg for various flap angles.

IV. Conclusions

A 16% thick supercritical airfoil with a trailing-edge flap was investigated in the IAR High Reynolds Number Two-Dimensional Test Facility at a chord Reynolds number of approximately 20×10^6. The investigation was carried out quite deep into the buffet regime and the effects of flap deflection on lift increment and buffet severity were analyzed. The results can be summarized as follows:

1) Buffet boundaries can be raised appreciably by positive deflections of the trailing-edge flap. The buffet onset boundaries for this supercritical airfoil occur very close to and in some cases correspond to $C_{L\max}$ when $M < M_{DES}$. To identify regions of different degree of severity in the C_L vs M plot, such as mild, moderate, and heavy buffeting as in coventional airfoils is not too meaningful.

2) The shock positions are determined from the steady-state C_p measurements. For Mach numbers near or less than the design value, the shock initially moves downstream with increasing angle of incidence to a maximum downstream position before moving slowly back upstream. For higher Mach numbers, only upstream motion of the shock is detected. At the lower Mach numbers, positive flap angles cause the shock to move further downstream while the opposite is true for negative flap deflections.

3) Spectral analyses of the balance normal-force outputs show shock oscillations at about 50–80 Hz between $M = 0.612$ and 0.792 inside the buffet regime. The magnitudes of the fluctuating normal force have quite large values near the "elbow" of the buffet onset curve. As the Mach number increases to higher values, the fluctuations in normal force decrease and the shock waves become more steady.

4) Excursion into the buffet regime and the resulting buffet severity can be represented either by the decrease in trailing-edge pressure ΔC_{pTE} or increase in magnitude of the fluctuating normal force $\Delta C'_N$. For Mach numbers near the design value, much larger changes in $\Delta C'_N$ with ΔC_{pTE} are observed than for other values of M. Whereas C_{pTE} decreases continuously with α, C'_N reaches a maximum and then decreases as the incidence is further increased except for high M where a maximum value in C'_N is difficult to determine. C'_N is a more accurate indicator of buffet severity.

5) At the design C_L, small flap angles do not increase the drag significantly for $M < M_D$. For off-design conditions ($C_L = 0.8$), the drag rise is much larger for negative flap angles than for positive angles of the same magnitude.

References

[1]Monaghan, R. C., and Friend, E. L., "Effects of Flaps on Buffet Characteristics and Wing-Rock Onset of an F-8C Airplane at Subsonic and Transonic Speeds," NASA TM X-2873, Aug. 1973.

[2]Friend, E. L., and Sefic, W. J., "Flight Measurements of Buffet Characteristics of the F-104 Airplane for Selected Wing-Flap Deflections," NASA TN D-6943, Aug. 1972.

[3]Eggleston, B., Poole, R. J. D., Jones, D. J., and Khalid, M., "Thick Supercritical Airfoils with Low Drag and Natural Laminar Flow," *Journal of Aircraft*, Vol. 24, June 1987, pp. 405–411.

[4]Lee, B. H. K., and Tang, F. C., "Transonic Buffet of a Supercritical Airfoil with Trailing-Edge Flap," *Journal of Aircraft*, Vol. 26, May 1989, pp. 459–464.

[5]Rabiner, L. R., Schafer, R. W., and Dlugos, D., "Periodgram Method for Power Spectrum Estimation," *Programs for Digital Signal Processing*, edited by The Digital Signal Processing Committee, IEEE Acoustic, Speech and Signal Processing Society, IEEE Press, New York, 1979, Chap. 2.1, pp. 2.1.1–2.1.10.

[6]Tang, F. C., and Lee, B. H. K., "Wind Tunnel Investigation of the Buffet Characteristics of a Supercritical Airfoil with Flap at a Reynolds Number of 20 Million," National Research Council of Canada, NAE-LTR-5X5/0179, Aug. 1988.

[7]Lee, B. H. K., Ellis, F. A., and Bureau, J., "Investigation of the Buffet Characteristics of Two Supercritical Airfoils," *Journal of Aircraft*, Vol. 26, Aug. 1989, pp. 731–736.

[8]Lee, B. H. K., "Oscillatory Shock Motion Caused by Transonic Shock-Boundary Layer Interaction," *AIAA Journal*, Vol. 28, May 1990, pp. 942–944.

[9]Blackerby, W. T., and Cahill, J. F., "High Reynolds Number Tests of a C-141A Aircraft Semispan Model to Investigate Shock-Induced Separation," NASA CR-2606, Oct. 1975.

[10]Lee, B. H. K., "Investigation of Flow Separation on a Supercritical Airfoil," *Journal of Aircraft*, Vol. 26, Nov. 1989, pp. 1032–1037.